ELECTRONICS AND ELECTRICAL ENGINEERING
ISSN 1392 – 1215 *2012. No. 6(122)*
ELEKTRONIKA IR ELEKTROTECHNIKA

TELECOMMUNICATIONS ENGINEERING
T 180
TELEKOMUNIKACIJŲ INŽINERIJA

A Concise Interference Model for Wireless Sensor Networks using Directional Antennas

K. Staniec, B. Miedzinski
Faculty of Electronics (K.S.), Faculty of Electrical Engineering (B.M.), Wroclaw University of Technology, Wyb. Wyspianskiego 27, 50-370 Wroclaw, Poland, phone: +48 71 320 34 34, e-mails: kamil.staniec@pwr.wroc.pl, bogdan.miedzinski@pwr.wroc.pl

crossref http://dx.doi.org/10.5755/j01.eee.122.6.1822

Introduction

A Wireless Sensor Network (WSN) starts with an unorganized deployment of physical sensors connected to transmit/receive modules. Such a system of sensors can be discussed in terms of a network only if logical and physical connections are established between these modules – a process called hence forth – the network spanning. There is a number of techniques for performing the self-organizing network formation, out of which the most popular to mention are the ZigBee-native algorithm and Stojmenovič family of algorithms. Invoking definitions from the theory of graphs, the former belongs to the group of, so called, Minimum-Spanning Tree (MST) whereas the latter are assigned to the Local MST (LMST) category (refer to [1–7] for more details on the subject of the spanning protocols and sensor networks for environmental monitoring). These methods, admittedly fast to perform in real networks, do possess some major drawbacks (exemplified in fig. 1a-c), namely they do not assure a reliable network structure and there occur crossings of connections between nodes pairs which makes the topology non-planar (a rather unwelcome feature of a WSN when directional antennas are in use). An improvement to these downsides can be made by incorporating techniques assuring a fully planar reliable structure based on the Gabriel's Graph (GG), as described in more detail in [9, 10]. One simple enhancement introduced there to the original GG is the way of choosing the neighbor to connect to. In the investigations presented in the following sections the neighbor was always found on the least-path-loss basis rather than first-to-respond basis. It means that even if many nodes respond to a connection inquiry issued by a node, the link will be set up only with the one(s) with the strongest radio signal. Such an approach is different from the typical one – as is the case with MST and LMST – where the choice is made on the first-to-respond basis. However, in practice the earliest replies do not necessarily arrive from the physically nearest devices (as, for example between nodes no. 17 and 20 in Fig. 1c).

Quantitative advantages of using: a) planar and b) reliable network topology as well as c) directional antennas for interference mitigation, have been thoroughly discussed in [9]. It was proven there that a substantial increase (c.a. 5 dB) in the average network SNIR (Signal-to-Noise and Interference Ratio) can be achieved as compared to networks spanned with the other two, common algorithms (MST, LMST).

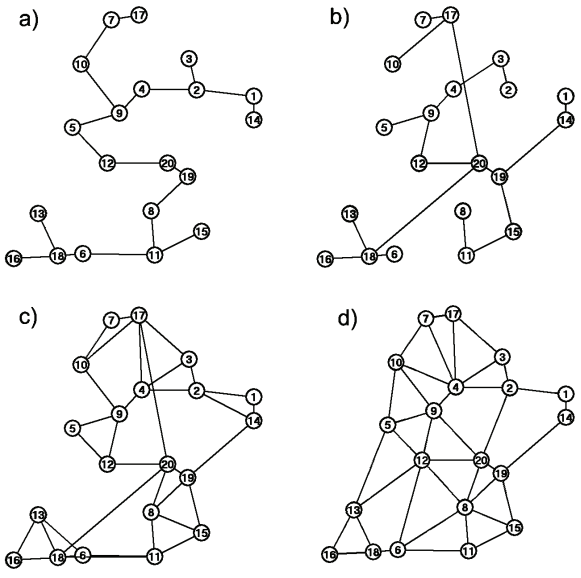

Fig. 1. Example of a WSN formed by a) MST algorithm; an LMST with b) short listen window and c) long listen window; d) planar algorithm. A case with 20 nodes

In the current paper it will be shown that if a sensor network is designed in accordance with these requirements (i.e. a-c), the relation between the desired signal received by a node and the sum of interference received from all

other nodes (so called Signal-to-Noise and Interference Ratio, or SNIR), exhibits a deterministic behavior which can be subjected to generalization in terms of a closed-form formula – an appreciable feature in real WSN design.

The origin of intra-network EMC issues in WSN

The occurrence of intra-network electromagnetic compatibility is an issue that needs to be accounted for with as much attention and priority as routing, medium access control procedures, security etc. It is so because excessive radio interference may lead to the cessation of the network operation, which event may take place when multiple sensors attempt to convey messages about a sensed phenomenon at the same time. Such a numerous and simultaneous detection and transmission may appear in situations of e.g. fire or flood. A common metric for expressing the link quality in digital systems is SNIR which value – as viewed by each node individually – determines whether the reception will be successful (if the current value of SNIR lies above its threshold level $SNIR_{thr}$) or failed (otherwise). For example, in a ZigBee IEEE 802.15.4 specification the minimum SNIR is defined as 5 dB [11, 12].

For the *k*-th node SNIR is given by (1), where *S* is the desired signal power in [W], *kB* – Boltzman's constant in [J/K], *T* – ambient temperature in [K], *BW* – channel bandwidth in [Hz], *NF* – Noise Factor [–], *M* – the total number of network nodes, whereas the last term in the denominator denotes the sum of radiations from all other nodes in the network (excluding, of course, the radiation from the *k*-th node for which SNIR is being calculated as well as an *m*-th node to which the transmission is addressed)

$$SNIR_k\,|_{[dB]} = 10\log\left(\frac{S}{N+\sum_i I_i}\right) = 10\log\left(\frac{S}{k_B\cdot T\cdot BW\cdot NF+\sum_{M/\{k,m\}} I_i}\right). \quad (1)$$

The simulation environment

For the purpose of network simulations a software simulator has been developed comprising two components (both described in [9, 10]):

- Matlab scripts (created by G. Debita) performing the network spanning algorithms on random scenarios generated by the C++ application described below;

- a C++ Builder application (created by K. Staniec) used for: a) generating random node distribution scenarios (ten scenarios for each number of nodes M, where M was varied from 10, 20 up to 100) to be fed into the Matlab scripts and b) calculating SNIR based on the output files generated by the Matlab scripts (as above).

Multiple scenarios have been generated for simulations, with a variable number of nodes, each located at 1.5 m above the ground and transmitting with the power 0 dBm (at 0 dBi of gain). Nodes have been scattered randomly over a square area of 500×500 m. For calculating propagation losses a two-slope (TS) model has been proposed for the radio signal attenuation between communicating nodes. The model is viewed as a solution better fitted to low-height sensor antennas than the pathloss formula proposed in [11] for low-rate WPAN (Wireless Personal Area Network), which appears to be too static and optimistic. In TS, the propagation losses follow a 20 dB per decade fade before the breakpoint distance, d_{brk}, and 40 dB per decade after, as given by (2) [13]

$$L = \begin{cases} 32.45 + 20\log f_{MHz} + 20\log d_{km}, & \text{for } d \le d_{brk}, \\ 20\log(h_1 h_2 / d^2), & \text{for } d > d_{brk}, \end{cases} \quad (2)$$

where $d_{brk} = \dfrac{4\pi h_1 h_2}{\lambda}$.

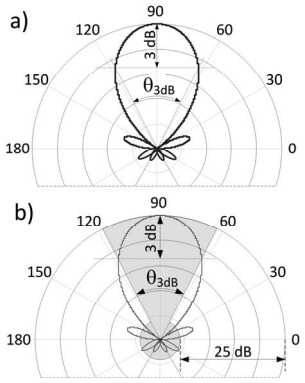

Fig. 2. A model of the antenna radiation pattern: a) exact; b) simplified

Simulations were carried out for sets of scenarios, each set consisting of ten scenarios of *M* nodes randomly deployed across the investigated squares area, with *M* varying from 10 to 100 (in steps of 10 nodes). A simplified model of a directional antenna was applied with a constant gain within the boresight (a 3-dB angle or θ_{3dB}) and attenuated by 25 dB outside, as in Fig. 2 [9, 10, 14–17].

Results of simulations: SNIR vs. antenna beamwidth

A set of curves has been obtained – each representing *SNIR* averaged over all generated scenarios for each particular value of *M*. It should be kept in mind that the figures presented herein refer to a statistical node and for individual nodes the calculated *SNIR* will occur at 50% chance. Nevertheless, the intention behind the simulations was to illustrate the general signal-to-interference tendency inside the network when directional (instead of omnidirectional) antennas are used. As can be seen in fig. 3a (more curves and their full analysis can be found in [9]), the most considerable change takes place when the network population is increased from *M*=10 to 30. With further increases in *M* the *SNIR* curves are shifted left less significantly. The interpretation of the outcomes is as follows: at a particular fixed beamwidth θ_{3dB} the *SNIR* experienced by a statistical node has a value depending on the number of network nodes – the greater *M* the lower *SNIR*, due to a growing number of possible interferes. What is also clear at first glance is a characteristic shape of

curves which will be given more attention in the section to follow.

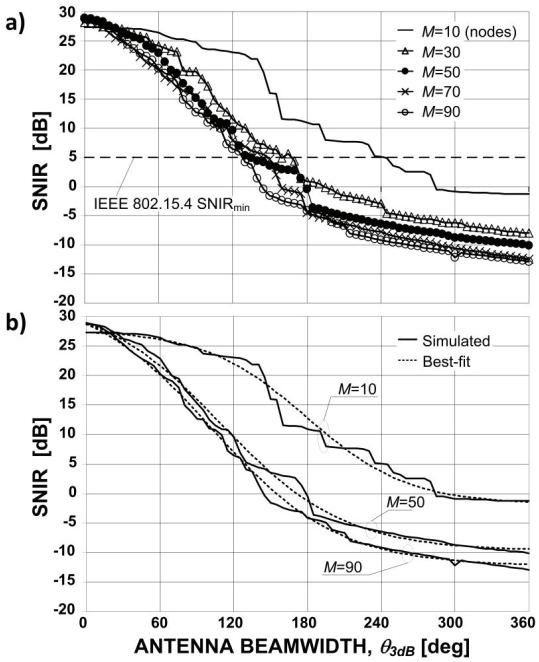

Fig. 3. A SNIR dependency on the antenna beamwidth, θ_{3dB} in planar WSN topology (a); simulated and best-fit curves for selected values of M (b)

A proposed formula for SNIR as a function of antenna beamwidth and network population

The shapes of curves shown in fig. 3a resemble an inverted logistic sigmoid function, defined – in its simplest form – by (3). In the methodology accepted in this paper, it was extended to a formula containing a set of five parameters $a_0(M)$–$a_4(M)$ for a proper modeling of each curve, as in (4), where M denotes the number of nodes, each set of parameters valid only for a specific M. For initial visual verification, three of the resultant modeled *SNIR* curves were graphically presented in for three selected values of M in fig. 3b. It can be seen that the achieved match is satisfactory when parameters are adjusted individually per curve – particularly in regions where the antenna beamwidth is smaller than 120° or greater than 240°. Moreover, it is easy to notice that as the best-fit parameters $a_0(M)$–$a_4(M)$ for all ten curves are plotted against M in fig. 4a, they exhibit some tendencies which lend themselves for being expressed in more generalized forms – of trends rather than of discrete values (as in fig. 4b).

The final aim the investigations presented in this section was, therefore, to determine and evaluate of a general closed-form formula relating *SNIR* to θ_{3dB}, valid for any M and given by (4). These best-fit sets of parameters $\hat{a}_0(M) - \hat{a}_4(M)$ obtained for each of the ten curves (for M=10–100) are depicted in fig. 4b:

$$y(x) = \frac{1}{1 + \exp(x)}, \tag{3}$$

$$SNIR(\theta_{3dB}, M) = \frac{\hat{a}_0(M)}{1 + \hat{a}_1 \cdot \exp\left[\hat{a}_2 \cdot \theta_{3dB} + \hat{a}_3(M)\right]} + \hat{a}_4(M). \tag{4}$$

Out of the five parameters (see fig. a), only $a_{1,M}$ and $a_{2,M}$ apparently not to vary with M therefore can be assumed constant. The other parameters, in turn, exhibit a linear ($a_{0,M}$, $a_{3,M}$) or exponential ($a_{4,M}$) dependency of M. With these observations in mind one can attempt to write general formulas for all parameters (now marked as $\hat{a}_0 - \hat{a}_4$ for better discrimination between the individually best-fit parameters and their generalized forms).

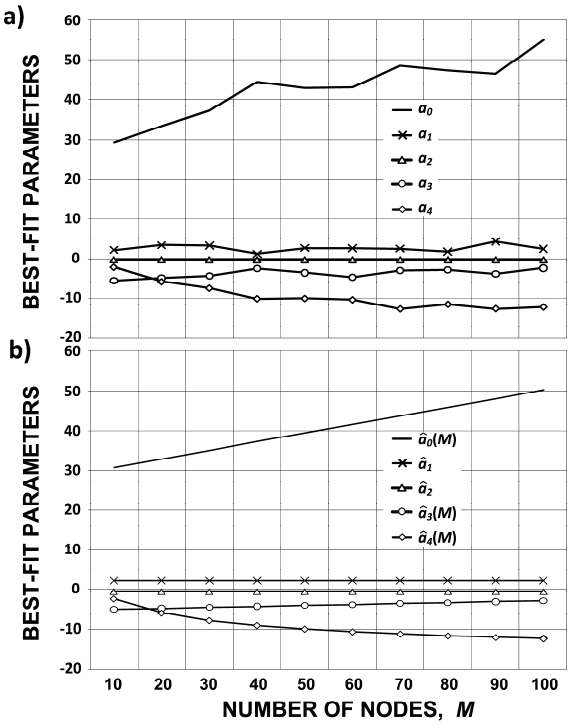

Fig. 4. Plots of individual parameter sets (a); generalized models of parameter sets (b)

The results of these generalizations are stated in Table 1. Since the fundamental part of research consisted in replacing individual sets $a_{0,M}$–$a_{4,M}$ with their generalized versions $\hat{a}_0(M) - \hat{a}_4(M)$ valid for any M, accuracy metrics were also placed in the last column of Table 1. For $\hat{a}_0(M)$, $\hat{a}_3(M)$ and $\hat{a}_4(M)$ the accuracy was expressed in terms of the correlation coefficient R whereas for the constant parameters $\hat{a}_1$, $\hat{a}_2$ the measure of fit was determined by the standard deviation σ_{dev} from the mean.

The simulations of *SNIR* were performed in 5° steps over the entire range of angles, which gave the total of 72 samples. For this number (<120) a t-Student distribution was applied to calculate the threshold R_{thr} above which the products of fitting can be regarded as correct. In the case of 72 samples R_{thr} should therefore be equal 0.232 for α=0.05, 0.302 for α=0.01 and 0.379 for α=0.001. As given in Table 1, even for the estimated $\hat{a}_3$ with the lowest R (0.685), it is still above the threshold R_{thr}=0.379 for α=0.001.

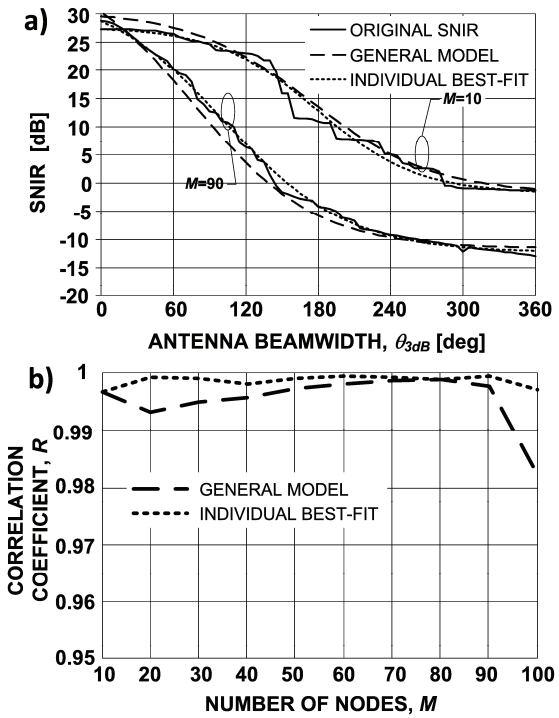

Fig. 5. Plots of individual and general best-fit parameter vs. original curves (a); correlation coefficients between the original SNIR curves vs. individual/general best-fits (b)

The last remaining step that consisted in recovering $SNIR(\theta_{3dB},M)$ from the generalized model using (4) along with its parameters in Table 1, and comparing it with individual *SNIR* curves obtained in the original simulations.

For purely visual comparison the accuracy of the reconstructed *SNIR* curves obtained with the general model for extreme values of *M*, can be verified in fig. 6a and Fig. 6b (for all numbers of nodes). The correlation coefficient *R* between the original simulated curves for each given *M* and those reconstructed from the general model defined in (4) and Table 1, is shown in fig. 5b. It is demonstrated here that regardless of *M*, the correlation always lies above 0.95.

Table 1. A set of generalized best-fit coefficients for SNIR dependency on *M*

Param.	*General form*	*m*	*n*	*k*	*Accuracy*
$\hat{a}_0(M)$	$m \cdot M+n$	*0.232*	*30.044*	—	*R = 0.934*
$\hat{a}_1$	*2.934*	—	—	—	σ_{dev} = *0.8779*
$\hat{a}_2$	*0.0199*	—	—	—	σ_{dev} = *0.0037*
$\hat{a}_3(M)$	$m \cdot M+n$	*0.024*	*-4.809*	—	*R = 0.685*
$\hat{a}_4(M)$	$n \cdot M^m+k$	*-0.25*	*41.246*	*-24.98*	*R = 0.984*

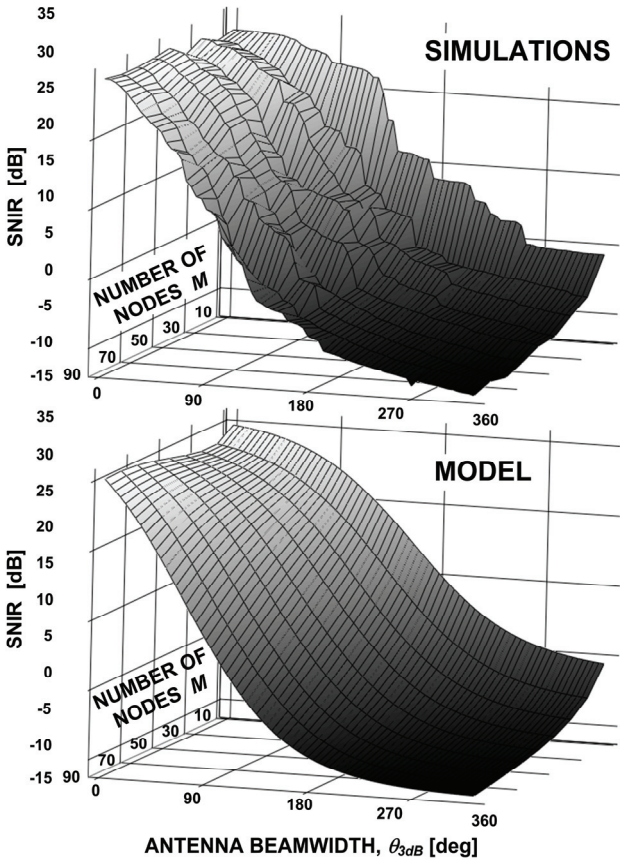

Fig. 6. Simulated SNIR (top) compared with the general model performance (bottom)

Lastly, it should noted that the model is based on some assumptions regarding the area size (namely 500×500 m) on which the nodes are located. However, as the side of the area is scaled from its original 500 meters down to 375 m and 250 m, a certain offset appears between the curves (see fig. 7) representing each dimension. It is the greatest (c.a. 4 dB) for θ_{3dB}=0° and gradually diminishes to zero as the beamwidth is increased (i.e. for θ_{3dB}=360° where all three curves overlap). Observing the response of (5) to its parameters $\hat{a}_0 - \hat{a}_4$ it can be easily proven that the initial value of *SNIR* (i.e. the offset discussed here) is only affected by $\hat{a}_0$. Therefore, for any other antenna heights and area sizes, the values given in table 1 need not be modified except $\hat{a}_0$ to fit the current value of *SNIR* for (θ_{3dB}=0°). More specifically, since $\hat{a}_0(M)$ changes in a linear fashion with *M*, for sensor configuration scenarios other (in terms of the area size and sensor heights) than those assumed in „The simulation environment“ section, $\hat{a}_0$ should be simply shifted by a constant offset up or down, whereas the other parameters in (5) will remain intact as in table 1.

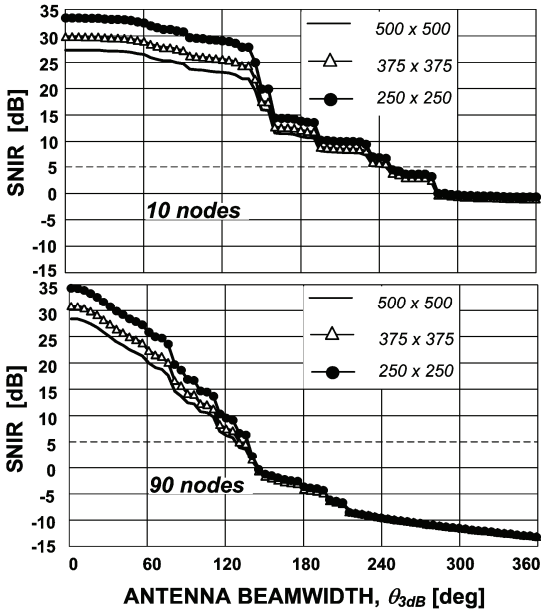

Fig. 7. Plots of individual SNIR curves for 10 and 90 nodes for different linear dimensions of the total square area

Conclusions

The paper was dedicated to the analysis of the radio-interference performance of a sensor network. Multiple simulations were carried out on various scenarios of sensor nodes placed randomly over a flat area and an average *SNIR* (per a statistical node) was obtained in each case. It was observed that in each case the signal-to-noise/interference ratio exhibited an inverted sigmoid shape. Moreover, as parameters of the best-fit curves have been adjusted for each simulated scenario separately, they also showed an apparent regularity of trends with M and θ_{3dB}. Remembering that the intra-network compatibility issue is critical to the network operation, a general formula for *SNIR* was derived and verified against the original separately obtained *SNIR* curves. It was found that the correlation coefficient estimations always lied above 0.95, which advocates the appropriateness of the derived general model.

It should be emphasized, that the values obtained from simulations as well as those modeled, represent an average value of *SNIR* in the WSN instead of referring to particular nodes. However, the sole purpose of the research was to demonstrate a general trend in interference improvement resulting from the application of directional antennas. Such an approach can be used for WNS's consisting of multiple nodes (and thus providing substantial redundancy) where individual treatment of nodes is cumbersome or even impossible.

Acknowledgements

This paper has been written as a result of realization of the project entitled: "Detectors and sensors for measuring factors hazardous to environment – modeling and monitoring of threats".

The project financed by the European Union via the European Regional Development Fund and the Polish state budget, within the framework of the Operational Programme Innovative Economy 2007÷2013.

The contract for refinancing No. POIG.01.03.01-02-002/08-00.

References

1. **Stojmenovič I.** Handbook of Sensor Networks – Algorithms and Architectures. – Canada: John Wiley & Sons, 2004.
2. **Gudzius S., Gvozdas V., Markevicius L. A., et al.** Real Time Monitoring of the State of Smart Grid Real Time Monitoring of the State of Smart Grid // Electronics and Electrical Engineering. – Kaunas: Technologija, 2010. – No. 10(106). – P. 57–62.
3. **Severdaks A., Supols G., Greitans M., Selavo. L.** Wireless Sensor Network for Distributed Measurement of Electrical Field // Electronics and Electrical Engineering. – Kaunas: Technologija, 2011. – No. 1(107). – P. 7–10.
4. **Gewali L., Mohamad K., Tun M.** Interference Aware Dominating Set for Sensor Network // Proceedings of Third International Conference on Information Technology: New Generations (ITNG'06), 2006. – P. 268–273.
5. **Xu W., Trappe W., Zhang Y.** Defending Wireless Sensor Networks from Radio Interference through Channel Adaptation // Proceedings of ACM Trans. on Sensor Network, 2008. – Vol. 4. – No. 4. – P. 18.1–18.34.
6. **Hekmat R., Van Mieghem P.** Interference power statistics in ad–hoc and sensor networks // Wireless Networks, 2008. – Vol. 14. – No. 5. – P. 591–599.
7. **Vakil S., Liang B.** Balancing Cooperation and Interference in Wireless Sensor Networks // Proceedings of 3rd IEEE Annual IEEE Communications Society Conference on Sensor, Mesh and Ad Hoc Communications and Networks (SECON), 2006. – Vol. 1. – P. 198–206.
8. **Zabasta A., Kunicina N., Ribickis L.** The Problem Issues of Intelligent Monitoring and Control of CIS in Latvia // Electronics and Electrical Engineering. – Kaunas: Technologija, 2012. – No. 2(118). – P. 57–62. DOI: 10.5755/j01.eee.118.2.1174.
9. **Staniec K., Debita G.** Interference Mitigation in WSN by Means of Directional Antennas and Duty Cycle Control // Wireless Communications and Mobile Computing, 2010. DOI: 10.1002/wcm.1089.
10. **Staniec K., Debita G.** Evaluation of Topological Planarity and Reliability for Interference Reduction in Radio Sensor Networks // EURASIP Journal on Wireless Communications and Networking. – Feb. 2012. – 2012:56. – DOI: 10.1186/1687–1499–2012–56
11. IEEE Std 802.15.4–2006, Part 15.4: Wireless Medium Access Control (MAC) and Physical layer (PHY) Specification for Low–Rate Wireless Personal Area Networks (WPANs).
12. CEPT, ERC Recommendation 70–03 Relating to the Use of Short Range Devices (SRD), Annex 1: Non–specific Short Range Devices. Version of 16 October 2009.
13. **Saunders S. R.** Antennas and Propagation for Wireless Communications Systems (2nd ed.). – Great Britain: John Wiley & Sons, 2007.
14. **Choudhury R. R., Vaidya N. H.** Impact of Directional Antennas on Ad Hoc Routing // Proceedings of IFIP Personal and Wireless Communications (PWC). – Sept. 2003. – Vol. 2775. – P. 590–600.
15. **Ramanathan R., Redi J., Santivanez C., Wiggins D., Polit S.** Ad Hoc Networking with Directional Antennas: a Complete System Solution // IEEE Journal on Selected Areas in Communications, 2005. – Vol. 23. – No. 3. – P. 496–506.
16. **Jasani H., Yen K.** Performance Improvement Using

Directional Antennas in Ad Hoc Networks // International Journal of Computer Science and Network Security, 2006. – Vol. 6. – No. 6. – P. 180–188.
17. **Dai N.** Throughput and Delay in Wireless Sensor Networks Using Directional Antennas // Proceedings 5th International Conference on Intelligent Sensors, Sensor Networks and Information Processing (ISSNIP), 2009. – P. 421–426. DOI: 10.1109/ISSNIP.2009.5416826.

Received 2012 04 04
Accepted after revision 2012 04 27

K. Staniec, B. Miedzinski. A Concise Interference Model for Wireless Sensor Networks using Directional Antennas // Electronics and Electrical Engineering. – Kaunas: Technologija, 2012. – No. 6(122). – P. 59–64.

The paper focuses on the issue of intra-network electromagnetic interference in wireless sensor networks where multiple sensor nodes are located on an open-space area at random locations. It is assumed that the topology is planar and reliable (i.e. at least two alternative paths exist for each node). Moreover, nodes are equipped with directional antennas for interference reduction. As is demonstrated, in such complex systems a statistical node will experience a regular dependency between the beamwidths of antennas mounted on sensor modules and the overall intra-network radio interference level. Based on the achieved simulated results, a simple formula has been proposed for expressing SNIR of a statistical (average) network node as a function of beamwidth and the number of nodes with a high correlation coefficient. As it turns out, there only of the model parameters is responsive to the scaling of size of the network area – it can be easily calculated then for any other size of the area than one presented in the paper. Ill. 7, bibl. 17, tabl. 1 (in English; abstracts in English and Lithuanian).

K. Staniec, B. Miedzinski. Kryptines antenas naudojančio bevielių jutiklių tinklo interferencijos modelis // Elektronika ir elektrotechnika. – Kaunas: Technologija, 2012. – Nr. 6(122). – P. 59–64.

Nagrinėjama intratinklo elektromangnetinė interferencija bevielių jutiklių tinkluose, kur jutiklių mazgai yra išdėstyti atsitiktinėse atviros erdvės vietose. Tiriama, kad topologija yra planarinė ir patikima (t. y. kiekvienam mazgui yra bent du alternatyvūs maršrutai). Be to, mazgai turi kryptines antenas interferencijai mažinti. Parodyta, kad tokioje sudėtingoje sistemoje statistinis mazgas bus priklausomas nuo jutiklių modulių antenų diagramų ir bendro intratinklo radiointerferencijos lygio. Remiantis gautais modeliavimo rezultatais, pasiūlyta paprasta formulė, išreiškianti statistinio tinklo mazgo signalo, triukšmo ir interferencijos santykį kaip antenos diagramos ir mazgų, turinčių didelį koreliacijos koeficientą, skaičiaus funkciją. Il. 7, bibl. 17, lent. 1 (anglų kalba; santraukos anglų ir lietuvių k.).